THERMO-IONIC GUN TEST FACILITY

A. Pisent, L. Rinolfi

Contents

page 1

1. Introduction

The LP group has started a consolidation program for the LPI machine. It includes the construction of a new LIL front-end as the leptons source for the LEP machine. A part of the LIL front-end is composed by the thermo-ionic gun and its associated modulator. It is followed by a focusing chamber which collects a maximum of particules with large emittances generated by the cathode.

Another part is the bunching system. In the light of the future developments, (LEP 200, B-Factory), it is foreseen to simplify the present LIL mechanics by using the previous LIL buncher W. This bunching system was design to bunch and accelerate to 4 MeV a beam of 1.5 A. The aim is now to adapt this structure to accelerate at the same energy a beam of 10 A.

In order to design the future LIL front-end, one of the facility to be built is the modulator for the e− gun and the corresponding beam diagnostic line. For time being,the gun geometry will remain unchanged. We describe below the design of the facility which will be installed in the Hall 162.

2. Lay-out of the test bench

Reference [1] describes the proposal for a new facility and figure 1 gives the lay-out of the test bench.

2.1   The gun

The gun is composed by a thermo-ionic cathode of 30 mm diameter with a spherical shape. It is followed by a grid at 1.5 mm downstream with the same shape. The grid is composed by a square mesh of 2.5 mm. At 26 mm downstream, there is the anode with a hole of 10 mm diameter which allows the electrons to go through it. The anode is at the ground potential.The cathode is at a DC potential of − 70 kV with a modulation of + / − 1 kV around it. It is tungsten made with impregnation of different material inside the metal. The cathode receives pulses at a frequency of 100 Hz. The grid remains at the constant potential of − 70 kV. The modulation of the cathode potential allows to produce electrons during the pulse when the cathode is negative compared to the grid. The difference of potential between the cathode and the grid is then roughly 500 V. With the new modulator, the cathode pulse length can be set between 2 and 60 ns. The electrons beam is submitted to an electrostatic field of about 5 MV/m.

2.2 The focusing chamber

Due to the large emittances coming out from the anode, a set of solenoids provide a strong focusing, optimized with the space charge effect, in order to collect a maximum of particules. Although the solenoids are shielded close the anode, one magnet is necessary to cancel correctly the magnetic field on the cathode. A electrostatic pick-up called ECM 01 is situated just downstream the first focusing solenoid and allows a current measurement.

2.3 The beam line

Downstream the focusing chamber,a vacuum valve allows to separate the vacuum gun from the rest of the line. A Wall Current Monitor could be installed inside the first solenoid followed by a set of steering dipoles. A second solenoid will contain the beam at high current and adjust the beam sizes either at the screen or at the Faraday cup. A system for the vacuum pump is installed before the tank which holds a scintillator screen. The end of the line receives the Faraday cup. Emittances measurements will be possible with the installation of a pepper pot not drawn on the figure 1.

2.4 The solenoids

Table I summarizes the characteristics of the solenoids installed on the test bench. All solenoids are water-cooled except SNA 01 which has an indirect water cooling. All are protected with thermo − contact and controlled by a flow meter. The alignment is made once mechanically. It is assume that the beam trajectory is on the magnetic axis.

3. Magnetic field.

3.1 Experimental measurements

Following a specification request, a note [2] summarizes the magnetic measurements made with the solenoids around the focusing chamber. Figure 2 gives the calibration curve for the SNA 01 coil used to cancel the magnetic field on the cathode. Figure 3 shows the magnetic field on the axis versus the longitudinal coordinate from the solenoid SNB 02 for two different currents. Figure 4 is the same for the solenoid SNC 02 and figure 5 shows the resulting magnetic field when both solenoids are excited. The superposition principle is verified over the whole range of current.

Reference [3] gives all the data. In table I is given the maximum field on the axis normalized to 1A circulating current.

3.2 Field calculations.

The solenoids SNF 03 and SNF 04 are identical type as SNC 02 but without magnetic shielding. The field has been calculated using the program ANSYS. Figure 6 gives the axial field for SNF03 as from simulations. The results are presented in the reference [4].

The magnetic field on beam axis for the case of a thick coil in the air can be calculated analytically; this method has been used for a fast preparation of the input for the programs that simulate the dynamics.

Table I

Kind	Aperture (mm)	Number of turns	Max.Current (A)	Resistance (m ohm)	B_{max}/I (Gauss/A)
SNA01	304	230	13	950	10.0
SNB02	21	109	150	47	15.72
SNC02	120	59	150	60	8.89
SNF03	120	59	150	60	4.34
SNF04	120	59	150	60	4.34

4. Beam Optics

4.1 General considerations.

The beam generated by the gun can be considered to be continuous and monoenergetic: the pulse at the grid is long enough to establish a condition of dynamical equilibrium. The transit time through the gap can be calculated in nonrelativistic approximation as[1]:

$$T = g\sqrt{\frac{2m}{eV_0}} \approx 0.3 \ nsec \tag{1}$$

where m is the electron mass, e is the elementary charge, $g = 2.75$ cm is the gap length and $V_0 = 70$ kV is the gun voltage; the time T has to be compared with the 20 nsec of the gun pulse.

The transverse dynamics in the test line is determinate by the external focusing forces (solenoids and radial component of E in the gun) and by the space charge. The grid at the cathode produces an emittance proportional to the emitting area and spherical aberrations are generated by the shape of the cathode.

For the calculation of beam envelopes two straight methods are known:

- the use of TRANSPORT matrices, for a beam with emittance and negligible space charge [5]: the transformation of the beam ellipsis in transverse phase space determinate the beam parameters at each z.

- the solution of the paraxial equation with space charge calculated in laminar approximation when the emittance can be neglected [6]: the laminar hypothesis implies that the most external trajectory remains on the envelope, making possible an exact evaluation of the space charge

---

[1] If we consider the potential to be linear in the gap region: $V(z) = V_0\frac{z}{g}$ the energy balance in the point z:

$$\frac{1}{2}m\left(\frac{dz}{dt}\right)^2 = eV(z)$$

gives by integration equation(1).

force acting on it.

The impact of each of those two approximations is extensively discussed in Appendix A. For the test line here described the space charge is important, and the emittance can not be neglected. It has then been necessary to use a multiparticle code (PARMELA). The solution calculated in laminar approximation turned out to satisfy also the complete problem.

4.2 Beam dynamics in laminar approximation (SOLOPT)

SOLOPT (SOLenoid OPTics) is a short code that tracks the beam through the transfer line using TRANSPORT matrixes for the solenoids and non-linear kicks for the space charge [7]. It assumes laminar motion, a continuous beam and no acceleration. SOLOPT has been written to calculate the beam dynamics of the photocathode test bench of CTF, where the small emittance generated by the photocathode justifies the laminar approximation [8].

As a zero order approximation we consider a layout constructed with geometrical optics methods (fig. 7) making use of the following assumptions:

- at the cathode the magnetic field is null.

- SNB02 and SNC02 are such that they keep the beam within the 5 mm of radius of the pipe between z_1 and z_2 and focalize it at F_3.

- SNF03 and SNF04 are thin lenses with focal length f given by:

$$f I^2_{coil} = \frac{4(B\rho)^2}{\int b^2 dz} = 181.1 \, m \, A^2 \quad at \quad 70 \, keV$$

Here $(B\rho)$ is the magnetic rigidity and $b = B/I$ is the longitudinal field generated by 1 A circulating in the coil.

The geometrical optics of fig.7 fits into the vacuum pipe, requires the same current in SNF03 and SNF04, and is well suited to host a 10 A beam. In fact, from the solution of the equation describing the envelope of a laminar beam in a drift space, it can be found that the maximum current that can be transmitted with a symmetrical configuration is [8]:

$$I_{max} = 1.1696 \frac{\pi (B\rho) \gamma^2 \beta^2}{\mu_0} \left(\frac{r}{z}\right)^2$$

where μ_0 is the magnetic permeability of vacuum, β and γ are the relativistic parameters, r and z are shown in fig.15. At 70 keV we have:

$$I_{max} = .79 \times 10^3 \left(\frac{r}{z}\right)^2 \, [A]$$

A maximum beam current of 10 A requires then $r = .113 \, z$. Our geometry fulfils this condition. We just observe that between SNB02 and SNF03 and between SNF04 and the Faraday cup the geometrical solution is not symmetric: the theory does not applies exactly, but gives anyway an idea of beam dimensions and solenoid spacing required.

Assuming in z_2 a parallel beam with radius 5 mm SOLOPT gives indeed a matched solution for a beam current of 10 A. In table II are given the solenoid currents for the geometrical solution (without

space charge and determining just SNF03 and SNF04 strengths) for a beam current of 3 A and 10 A; the first value is close to the LIL current for LEP operation, the second is the goal of the new bunching system. In fig. 8 is plotted the beam behavior for the last two cases.

Table II

	Geom. Optics	$I_{beam} = 3A$	$I_{beam} = 10A$
I_{coil} in SNB02 (A)	–	57.3	63.6
I_{coil} in SNC02 (A)	–	101.2	112.5
I_{coil} in SNF03 (A)	54.9	64.9	64.9
I_{coil} in SNF04 (A)	54.9	60.2	60.2

4.3   The electron dynamics in the gun (EGUN)

EGUN [9] is a well known code written to study the optics of an electron continuous beam, with special attention to gun optics design. The main parts are a Poisson solver and a ray tracker, plus various routines to simulate the effect of an external magnetic field; the code calculates the field without particles, tracks the particles in that field (considering also the external B field), recalculates E in the presence of the particle distribution and retracks the trajectories, and so on until the result converges.

We have implemented in EGUN the geometry of the new gun for LIL; the shape of the electrodes is the same as for the present gun designed by CGR McV. In fig.9 this geometry is shown; 10 equipotential lines and 50 trajectories are tracked. The grid surface is considered uniformly emitting electrons with $\gamma = 1$.

At the cathode surface the space charge of the already emitted electrons limits the current to a maximum value I_{max}; the perveance, defined as:

$$K = I_{max} V_0^{-\frac{3}{2}} \qquad (2)$$

expresses this limit as a function of the gun voltage V_0. Our calculations give a perveance:

$$K = 0.79 \times 10^{-6} \left[A\ V^{-\frac{3}{2}} \right]$$

In the plot of the transverse phase plane the effect of spherical aberration can be seen; the most external trajectories are overfocused. As a result the emittance calculated at $z = 52$ mm is 393π mm-mrad. The electron produced in the most external part of the cathode are lost very soon in the line. We have concluded that an emittance of 100 π mm mrad and a current of 10 A are a reasonable input for PARMELA at $z = 52$mm. At lower current the overfocusing produced by the electrostatic field is bigger, so that the transmission is worse (fig. 10).

In this modellization the effect of the grid is not considered; in Appendix B we present a very crude treatment of the problem. It gives an idea of the influence of grid geometry and position on final emittance; the emittance growth due to the grid is generally of the same order than the one created by spherical aberration. Both those effects give a worst emittance as we decrease the current from the maximum one. For gun designing a careful modellization of the grid is needed; for the simulation of

the bunching system of LIL the results of emittance measurements will be precious to determinate the initial beam characteristics.

4.4 Beam dynamics with space charge and emittance (PARMELA).

PARMELA is a multiparticle code developed at LANL to calculate electrons dynamics in the presence of space charge; the version installed at CERN on CRAY machine is directly derived from the LAL version (running under VAX) [10]. A sample of macroparticles is randomly generated in six dimensional phase space, according to given emittance, ellipsis orientation and reference particle coordinates at time zero. The time evolution of those particles is then calculated taking into account external forces (magnetic focusing and RF fields) and space charge forces, calculated on a mesh travelling with the reference particle.

The choice of PARMELA to calculate the test line has been done mainly to gain confidence with a program well suited also for the next calculations of the bunching system. In this framework in Appendix A is extensively treated the simple case of a drift space.

The test line has been simulated for the two currents (after the anode) of 3 and 10 Amps; the initial emittance has been varied between 2 and 200 π mm mrad. We underline that this is the value of the 100% emittance, i.e. the area of the ellipsis in xx' phase-plane that includes all the macroparticles. For the distribution chosen by PARMELA (a uniform distribution over an hyper−ellipsoid in the 4D transverse phase space) the 100% emittance is equal to 6 times the r.m.s. emittance, defined as:

$$\varepsilon_{r.m.s.} = \sqrt{\overline{x^2}\,\overline{x'^2} - \overline{xx'}^2}$$

where the bar indicates the average over the particle distribution.

The results found are in a good agreement with those calculated in laminar approximation, also for the bigger emittances, where the approximation is worse. For an initial value $\varepsilon = 100$ π mm mrad the transmission of electrons is maximized by the solenoid strengths of Table II (determined by running SOLOPT).

In table III we show the final emittance r.m.s. and the transmission for various initial emittances. The transmission is defined as the ratio between beam current at z = 52mm and at the Faraday Cup; z = 917mm and z = 1298mm are the two extreme positions of the Faraday Cup. The emittance growth is due to the non-linearity of space charge forces; between the first and the second position of the Faraday cup the emittance r.m.s. decreases because the most external particles are lost.

In figure 11 and figure 13 the envelopes and the initial and final phase plane are shown for the two currents of 3 and 10 A and for an initial emittance of 100π mm mrad.

Table III

Gun current (A)	Faraday Cup position (mm)	Gun emittance (mm mrad) 50π	100π	200π
3	917	87%(86π)	88%(89π)	88%(95π)
"	1298	74%(62π)	75%(61π)	74%(65π)
10	917	65%(218π)	64%(224π)	60%(205π)
"	1298	35%(84π)	32%(80π)	30%(82π)
		Transmission[%] (final emittance r.m.s. [mm mrad])		

5. Beam parameters to be measured.

5.1 Maximum current from the gun

A new modulator being installed, it is primordial to know what are the limitations in current coming out from the gun. It is expected to run routinely with a current of 10 A which means to have currently 15 A downstream the focusing chamber. This will be measured mainly with the electrostatic P.U. ELM 01.

5.2 High Voltage tests.

The gun modulator is designed for a nominal value of 80kV between the cathode and the anode. However the hardware is built to support 100kV. Several tests will be performed in order to find a good compromise

between hardware constrains (minimum voltage) and reduction of space charge effect (maximum voltage).

5.3 Beam transport of 10 A

The modellisation has shown that it was possible to transport 10 A with the designed optics and the corresponding currents in the solenoids. A screen MTV will allow to check the transverse dimensions of the beam and the Faraday cup to check the maximum current received at the end of the line.

5.4 Emittance measurements

The study of the bunching system (done with the help of the code PARMELA) [11] has needed the emittance of the 70 KeV beam as an input. The experimental measurements of this quantity is then of great importance.

It is foreseen to do emittance measurements based on the pepper pot principle. A rough estimate could be done with the Faraday Cup. We expect to verify the emittance values used to design the new

buncher configuration.

5.5 Effect of the distance between the grid and cathode

Formula (6) in appendix B shows that the current is inverse proportional to the distance and proportional to the 3/2 power of the potential between cathode and grid. Although it is not obvious to measure this latter we intend to verify this law concerning these 2 parameters.

6. References.

1.   L. Rinolfi "Proposition pour une installation d'essais" Note manuscrite 1/02/1989

2.   D. Cornuet "Proposition de mesure magnetique du systeme de focalisation du canon a electrons du LIL" PS/PA Note 89-24

3.   D. Cornuet G. Patron Resultats des mesures magnetiques (to be published).

4.   F. Rohner "Solenoid for the LIL Canon Magnetic calculation with ANSYS" PS/PA Note 89 – 36

5.   A.P. Banford 'The Transport of Charged Particles Beams', E.& F. N. Spon Limited (1966)

6.   J.D. Lawson, 'The Physics of Charged-Particles Beams', Clarendon Press, Oxford (1978) pag. 118

7.   A. Pisent 'SOLOPT: a Transport code with space charge in a solenoidal field,Note PS/LP 89-29

8.   Y. Baconnier, A. Pisent, 'CLIC Test Facility: the Photocathode Test Bench', Clic Note 104 (1989)

9.   W.B.Hermannsfeld, SLAC-331 (1988)

10.   B. Mouton "PARMELA" LAL internal report.

11.   A. Pisent L.Rinolfi note under preparation.

12.   H. K. Wolkstein 'Design considerations for grid-controlled electron guns for pulsed traveling-wave tubes' RCA review, sept. 1960 Volume 21.

Appendix A

Emittance and space charge influence on the envelope of a drifting beam.

For a laminar beam the most external trajectory coincides with the envelope and the equation of motion in a drift space can be solved in the presence of space charge (an average angular momentum respect to the beam axis equal to zero is assumed). If at $z = 0$ the beam has radius r_0 and is parallel to the axis, it will have radius r and maximum divergence r/z when [8]:

$$I_b = a\left(\frac{r}{z}\right)^2 \quad with \quad a = 1.1696\frac{\pi(B\rho)\gamma^2\beta^2}{\mu_0} \tag{3}$$

where I_b is the beam current; moreover in this conditions $r_0 = .43r$. In fig.15 the geometrical meaning of r,r_0 and z are shown.

Let's now consider a beam without space charge represented in $z = 0$ by the ellipsis of equation:

$$\left(\frac{r}{r_0}\right)^2 + \left(\frac{r_0 r'}{\varepsilon}\right)^2 = 1$$

the main axis are parallel to the coordinate axis $r = 0$ and $r' = 0$ (in TRANSPORT language $\alpha = 0$) and ε is the geometrical emittance. The equation of the envelope r as a function of z is:

$$\left(\frac{r}{r_0}\right)^2 = 1 + \left(\frac{z\varepsilon}{r_0^2}\right)^2 \tag{4}$$

To have an idea of when the envelope growing due to emittance and space charge are comparable, let's impose to the envelope (3) to pass for the two points $(z = 0, r_0)$ and (z,r). By imposing $r_0 = .43r$ the following result is found:

$$\frac{\varepsilon}{z} = \frac{.3882}{a}I_b \tag{5}$$

This result can be read in the following way:

$$If \quad \frac{\varepsilon}{I_b z} \ll \frac{.3882}{a} \quad \text{the laminar approximation is adequate}$$

$$If \quad \frac{\varepsilon}{I_b z} \gg \frac{.3882}{a} \quad \text{the TRANSPORT approximation is adequate}$$

It has to be reminded that a is proportional to $(\beta\gamma)^3$, so that increasing the energy the space charge can very soon be neglected.

With Parmela we have run the case:

$r_0 = 5mm$

$r = 11.6mm$

$z = 189mm$

$I_b = 3A$

$eV = 70KeV$

being this at the same time a check for the program (at very low emittance we know the exact equation for the envelope) and a verification of this approximate approach. In figure 15 we show the laminar solution calculated by SOLOPT.

For these values equation (4) gives an emittance of 280 π mm mrad to have an effect of the same magnitude from space charge and emittance. In table IV are shown the value of the envelope r at z for different emittances; it has been used the 100% envelope, i.e the maximum radius in the sample of macro-particles. This is the right value to be compared with the laminar solution, but gives an overestimation of the physical dimensions of the beam. In the simulations of the test line the 90% envelope (radius containing 90% of the macroparticles) has been used.

Table IV

emittance ε (π mm mrad)	envelope 100% r (mm)
2	12.7
20	12.7
200	14.6

Appendix B

The emittance generated by the grid.

The theory of a spherical Pierce cathode with electron emission controlled by a grid is extensively discussed in reference [12] where fig. 17 can be found; in this appendix we extend the theory to give an estimate of the emittance produced by the grid.

In a spherical cathode the equipotential surfaces (solution of Laplace equation without grid) near the emitting surface are almost concentrical spheres; the grid is located on one of these surfaces, let's say at potential Φ. In first approximation we can say that the effect of the grid is to force this surface to a potential V_g; if this potential is lower then Φ, the grid will limit the electron current by space charge effect according to:

$$I_b = \frac{2.335 \times 10^{-6}}{d^2} V_g^{\frac{3}{2}} S \tag{6}$$

where everything is expressed in MKS units, S is the cathode surface, d is the distance between cathode and grid. In this equation and in the following ones cathode and grid are approximated by parallel planes.

Until now we have considered the grid to be an equipotential foil permeable to the electrons; in the reality it is formed by a certain number of wires, spaced by Δl. Each hole between wires can be considered as a thin focusing lens of focal length:

$$f = \frac{2V_g}{E_2 - E_1}$$

where E_2 is the accelerating field at the grid and $E_1 = V_g/d$ is the field between cathode and grid. If we suppose the electrons to start parallel form the cathode, immediately after the grid the transverse phase plane will look like in fig.18, so that the geometrical emittance will be:

$$\varepsilon_{geom} = \frac{x_{max}\Delta l}{4d}\left|1 - \frac{E_2}{E_1}\right| \tag{7}$$

and the invariant emittance $\varepsilon = \beta\gamma\varepsilon_{geom}$. The emittance after the grid is proportional to the ratio between wires spacing and cathode-grid distance, to the grid area and to the relative step in the accelerating field. Lower currents do give bigger emittances (once fixed the geometry). At $V_g = \Phi$ the grid is transparent (except for the scattering on the wires).

We can do the following reasonable approximations:

• The field immediately after the grid is independent of the polarization voltage V_g, namely:

$$E_2 = \Phi/d$$

• the side x_{max} of the equivalent square grid used in (7) is the square root of the actual cathode area:

$$x_{max} = \sqrt{S}$$

- at the potential of the grid (around 500 V) we can use the non relativistic approximation:

$$\beta\gamma = \sqrt{\frac{2eV_g}{mc^2}}$$

Then the following system gives the emittance as a function of the beam current:

$$V_g = \left(\frac{I_b}{S}\frac{d^2}{2.335\times10^{-6}}\right)^{2/3}$$

$$\varepsilon = \frac{\sqrt{S}\Delta l}{4d}\frac{\Phi - V_g}{V_g}\sqrt{\frac{2eV_g}{mc^2}}$$

(8)

The only unknown parameter, the potential Φ, can be calculated form equation (6). Indeed from the EGUN run we know the space charge limited current for the gun I_{max}, and under this condition $V_g = \Phi$. Once assembled the gun, Φ can be measured as the value that maximize gun current.

For LII, gun we have used the following parameters:

$d = 1.5\ mm$ $V_0 = 70kV$

$\Delta l = 2.5\ mm$

$S = 10\ cm^2$ $I_{max} = 15A$

In table V are shown potentials and emittances as a function of beam current.

Table V

beam current I_b (A)	polarization voltage V_g (V)	inv. emittance ε (π mm mrad)
15	595	0
12	513	95
10	454	173
5	286	477

Figures

Figure 1:   Lay-out of the test bench.

DESSIN, RUGOSITE, TOLERANCES
SELON NORMES ISO

Figure 2: Calibration curve for SNA01
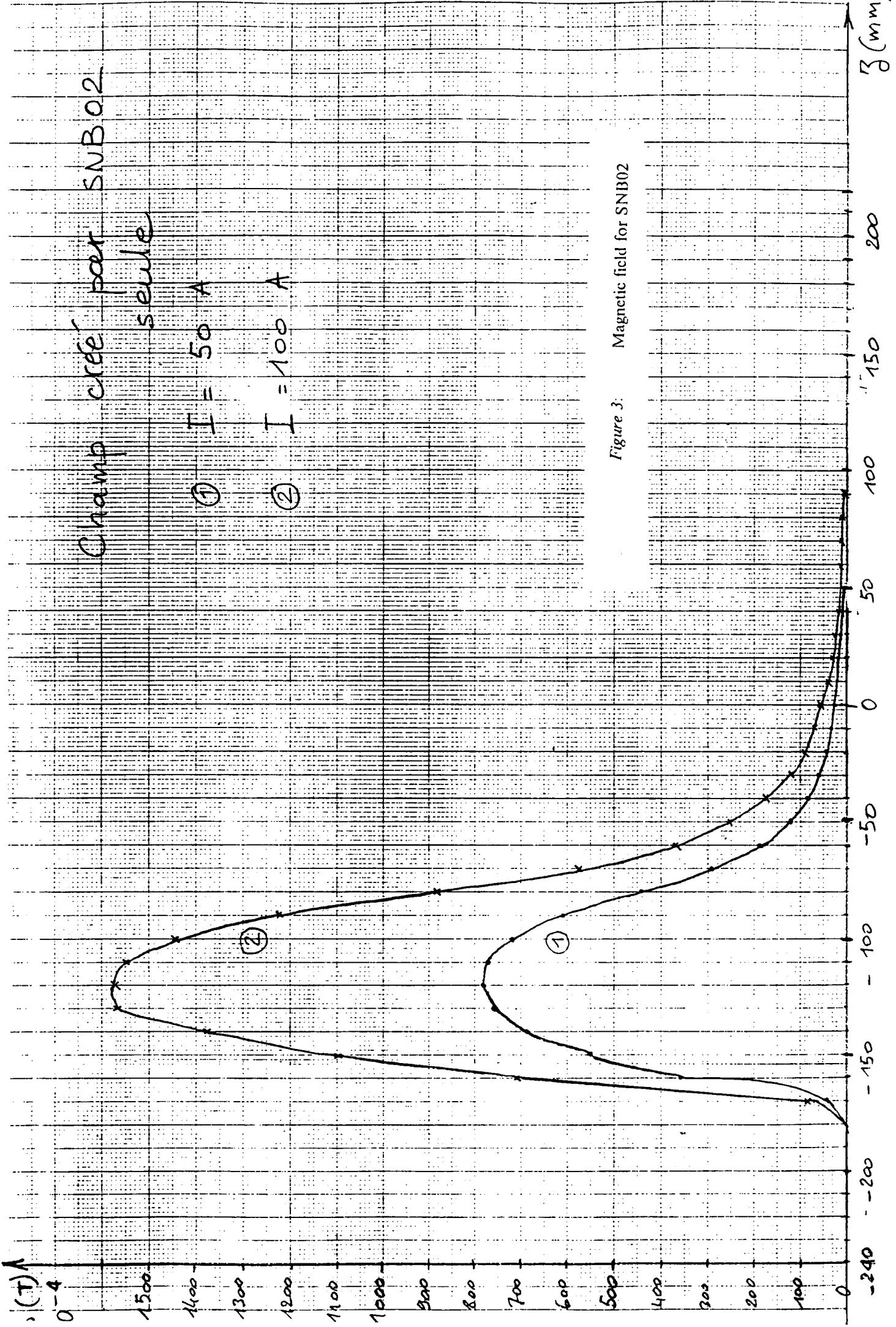
Figure 3: Magnetic field for SNB02

Fig. 3
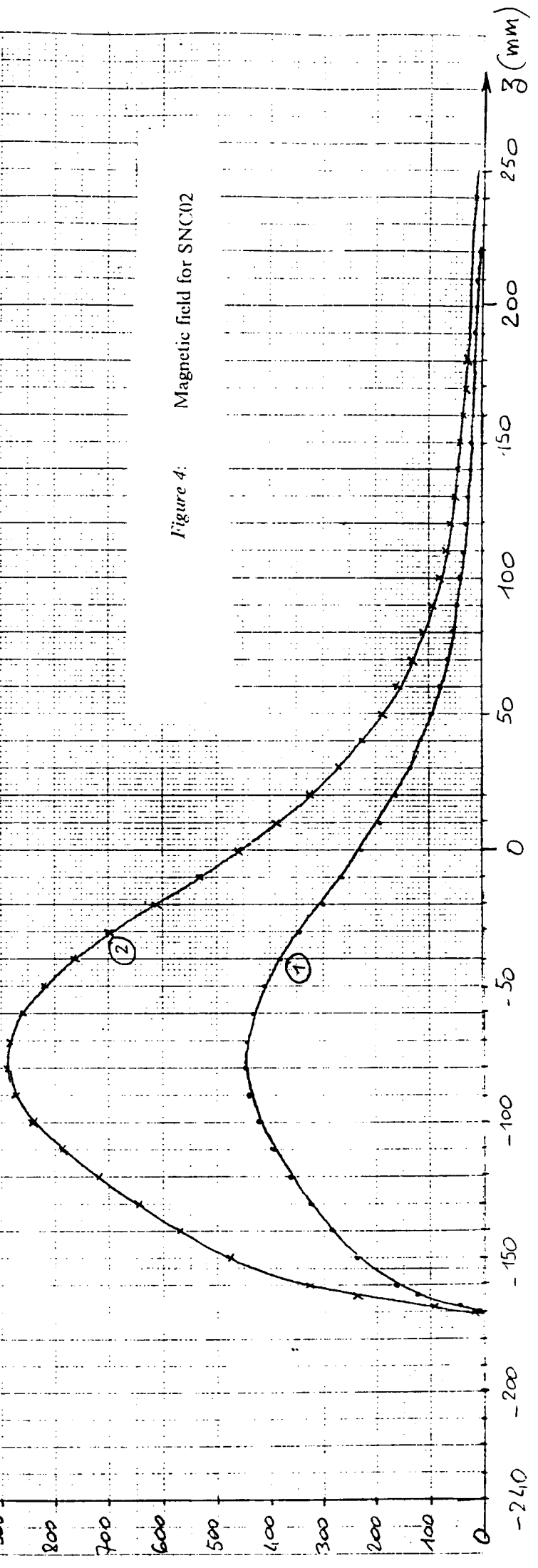
Figure 4: Magnetic field for SNC02
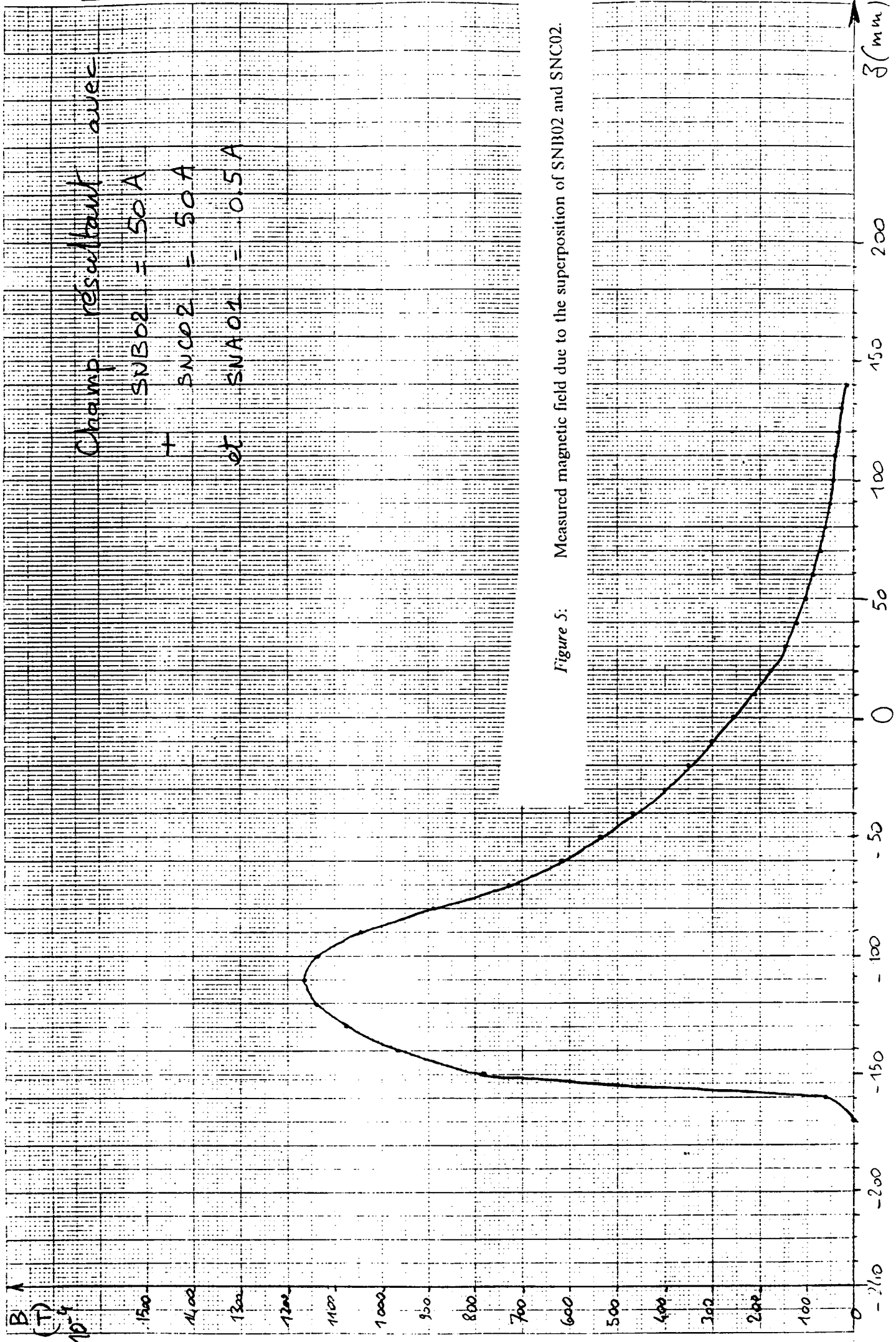
Figure 5: Measured magnetic field due to the superposition of SNB02 and SNC02.
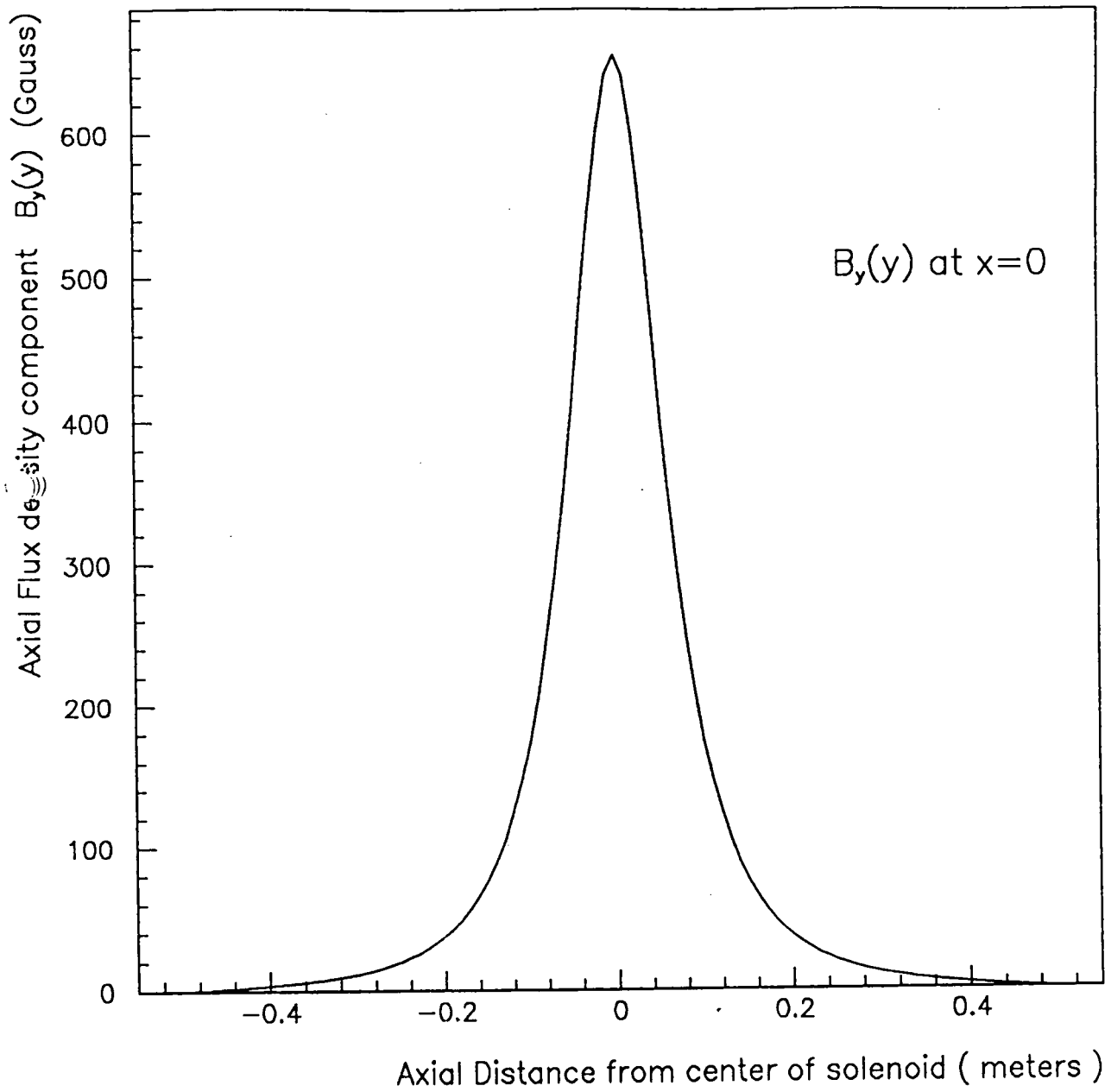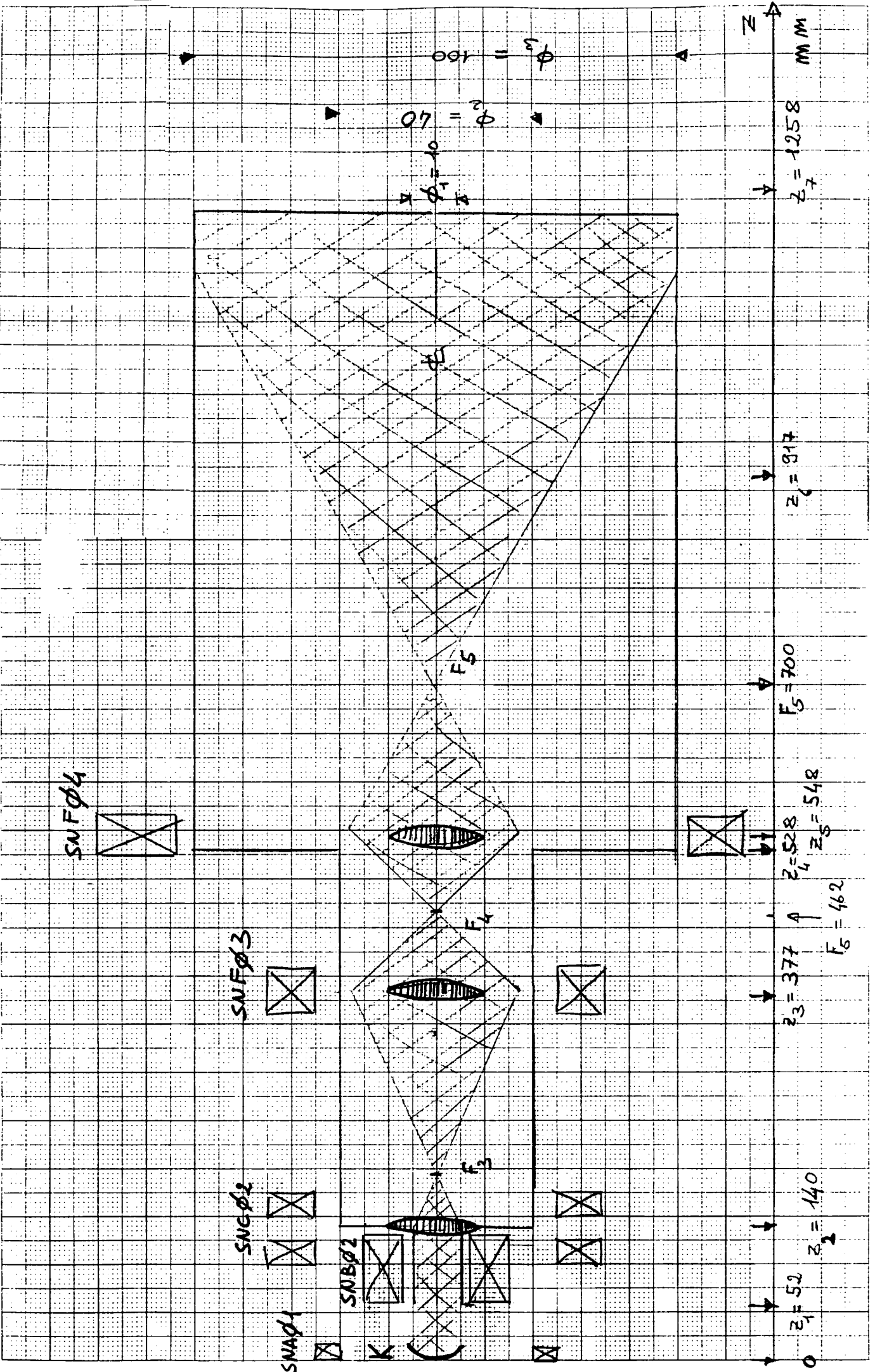
Figure 6: Calculated magnetic field for SNF03 (and SNF04)

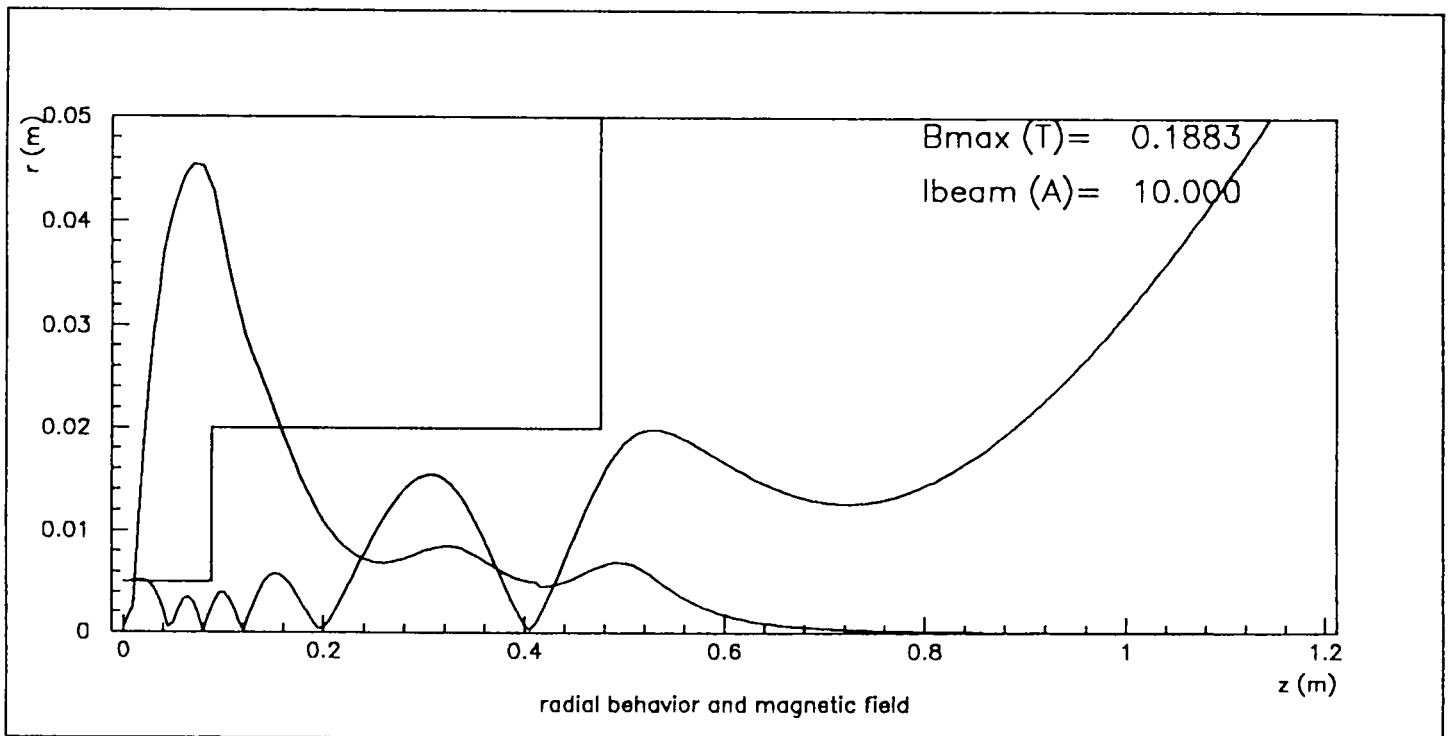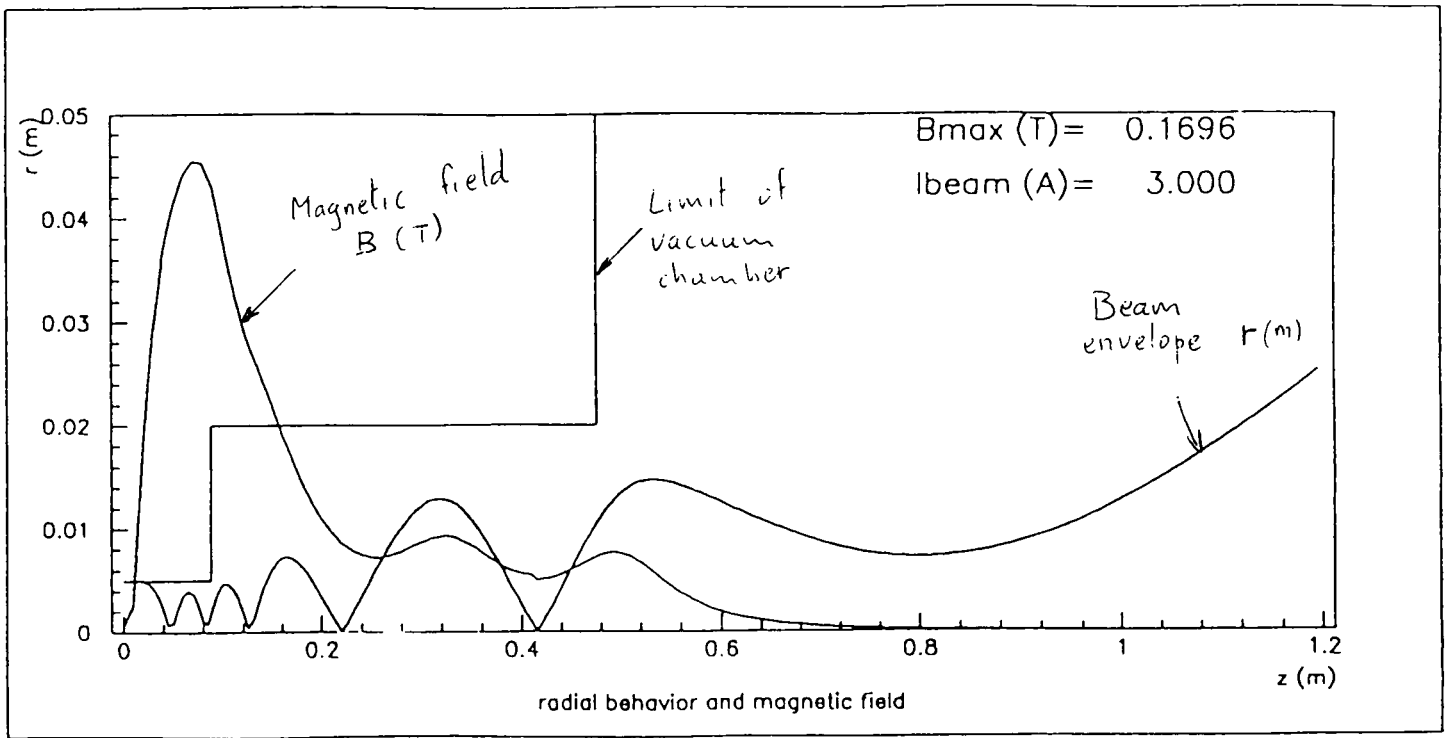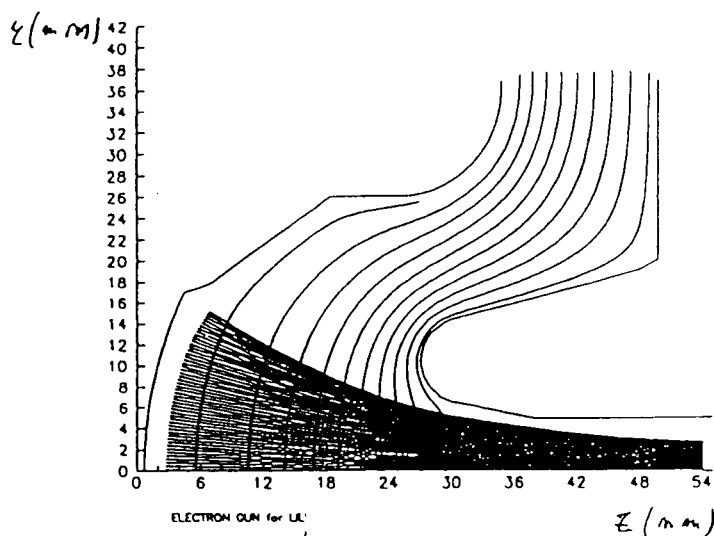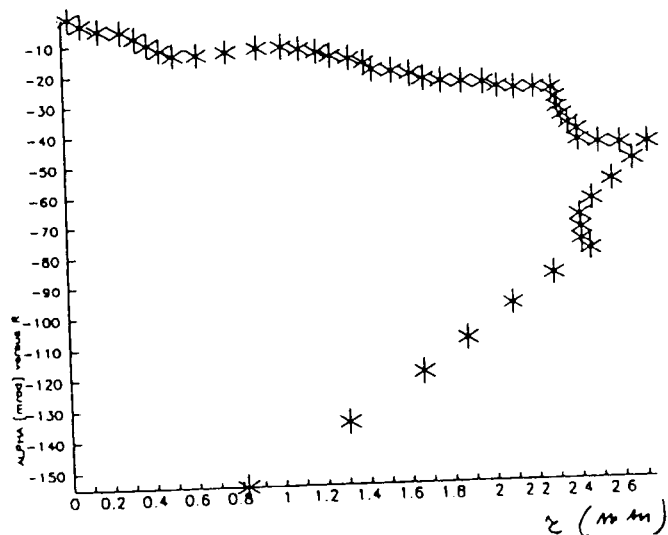Figure 7: The beam line and the geometrical solution.

Figure 8: Laminar solution for a beam current of 3 and 10 A.

$y\left(\text{* } m\right)$

a) Trajectories from the cathode to the anode output.

b) Phase space at the anode output.

Magnetic field
B (T)

2 FEB 90, 11:49, INTERACT 0 CERNVM
UNIT= 0.00100OM, STEP= 0.800, SPC= 0.500, MAGORD= 8, INTPA=F, MAGMLI

r
mm)

ELECTRON GUN

B(Z) GAUSS
I = 14.728 AMPS, PERV = 0.79512 MICROPERVS, 10 ITERATIONS.

$Z\left(m\,m\right)$
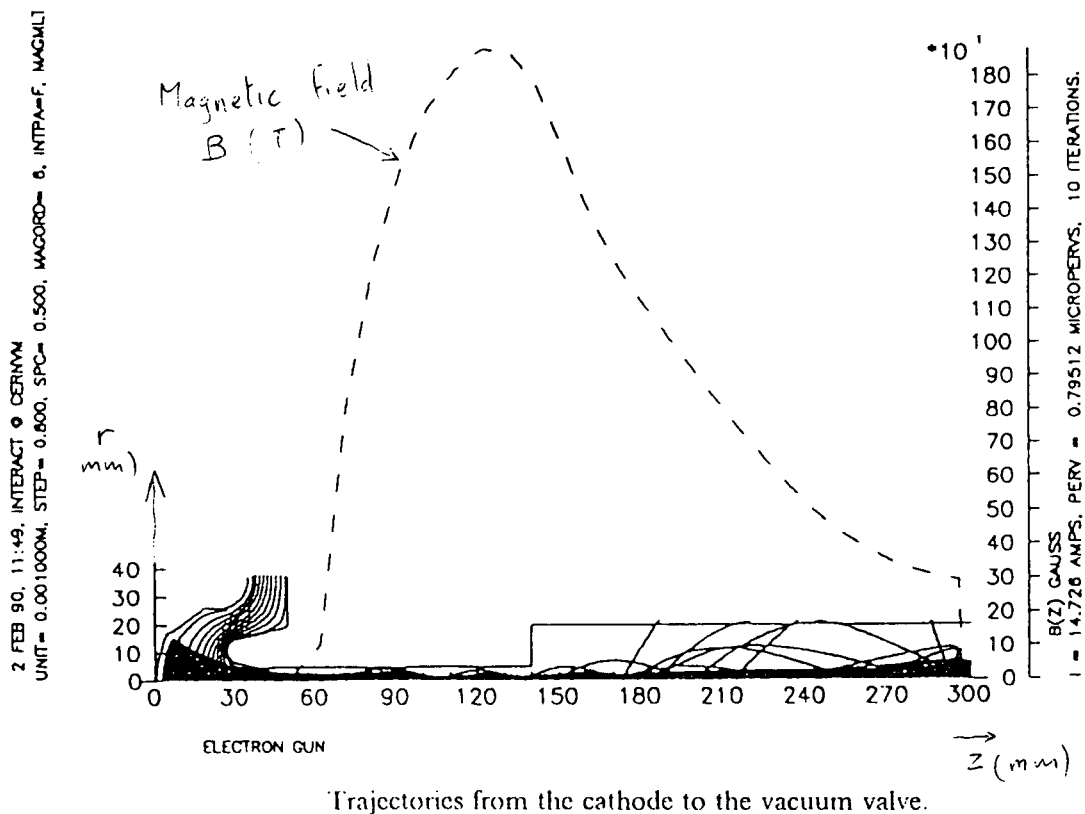
Trajectories from the cathode to the vacuum valve.

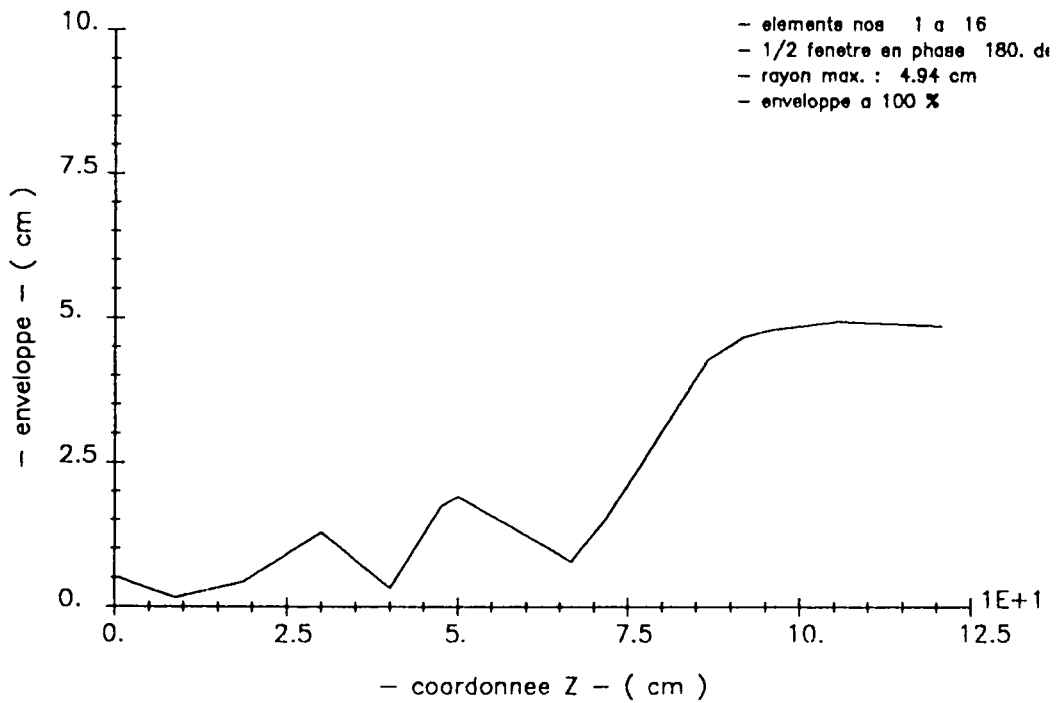*Figure 9:* Output of EGUN for space charge limited current. 15 A at the cathode.
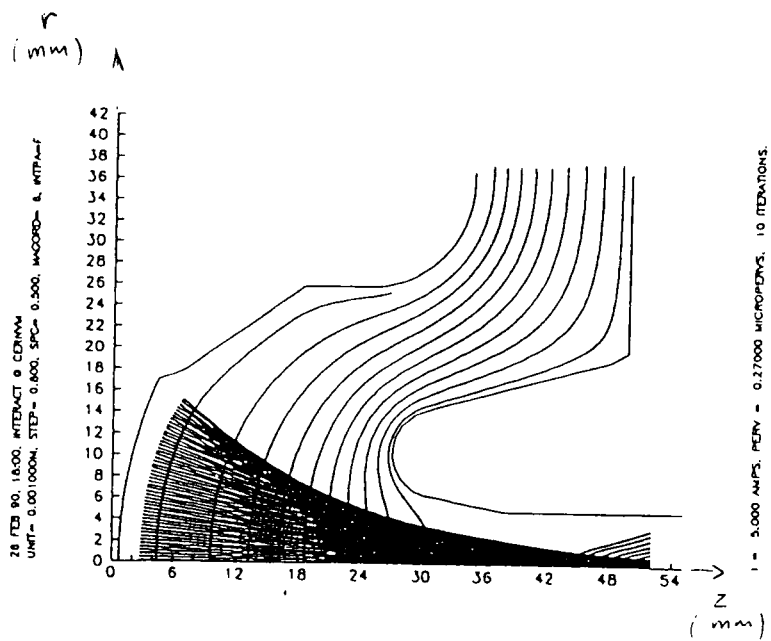
a)Trajectories
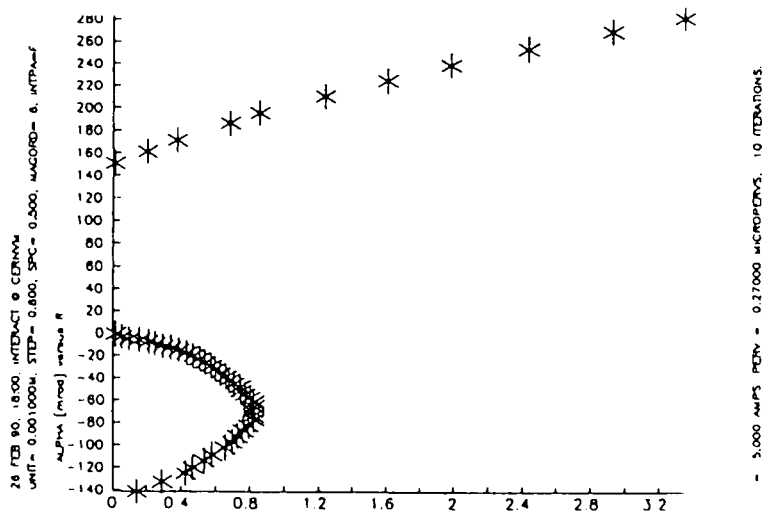
b)Phase space

Figure 10:   Output of EGUN for a current of 5A at the cathode.

- elements nos 1 a 16
- 1/2 fenetre en phase 180. d
- rayon max. : 2.38 cm
- enveloppe a 90 %
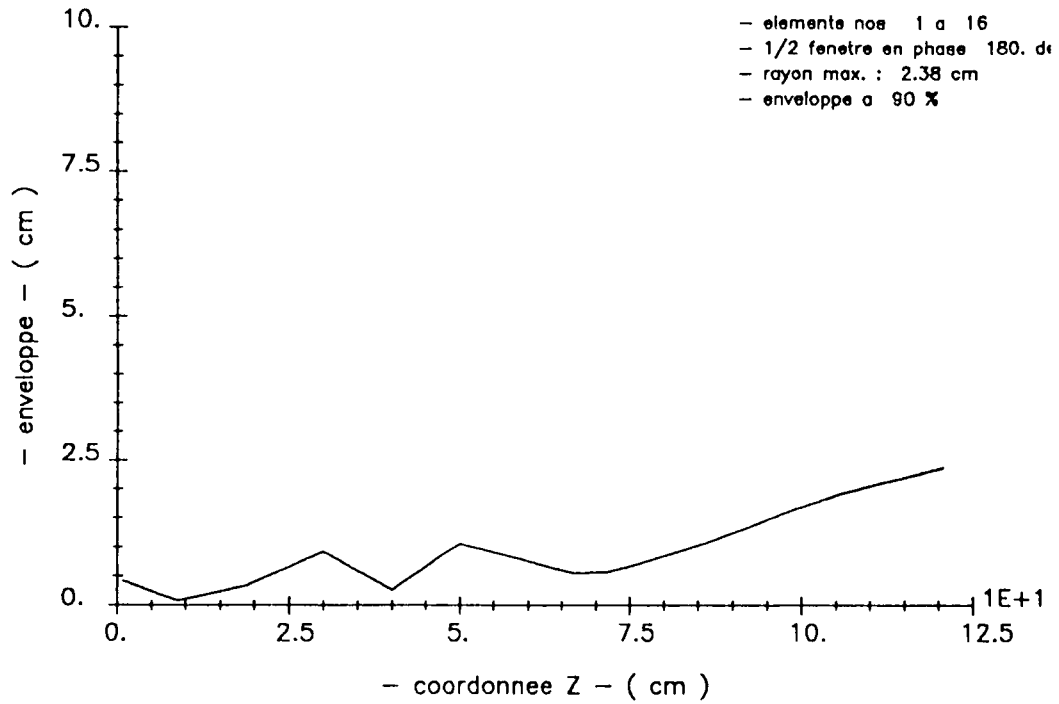
a) Envelope with 90% of particles

26.03.90

- elements nos 1 a 16
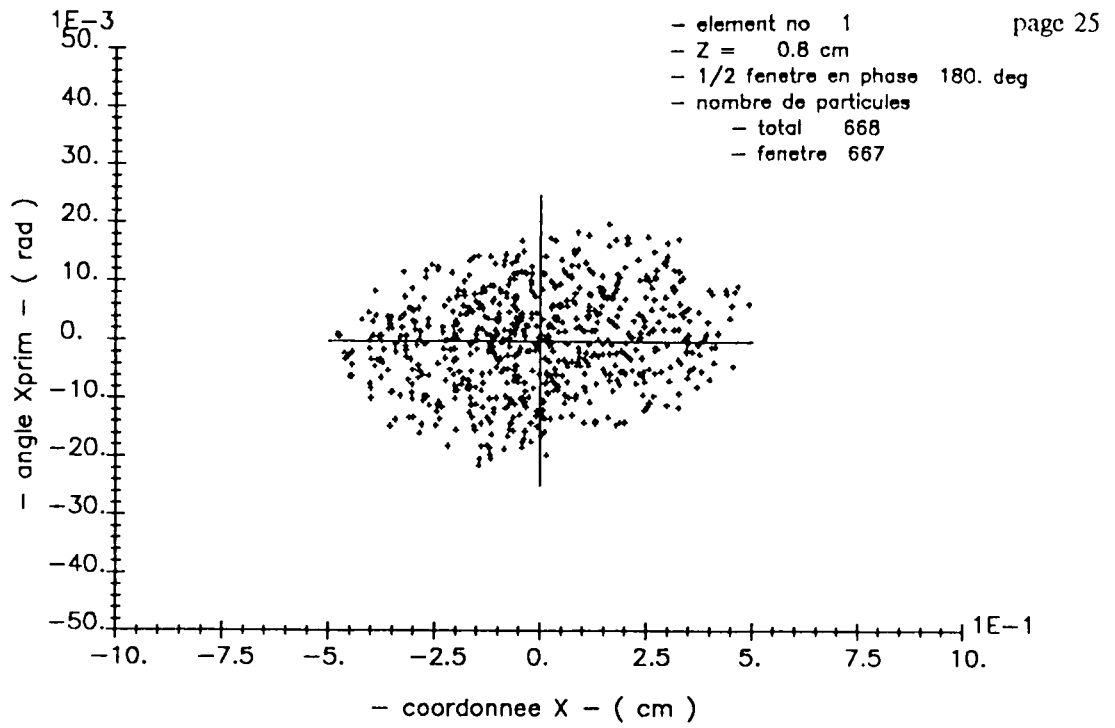- 1/2 fenetre en phase 180. d
- rayon max. : 4.94 cm
- enveloppe a 100 %

26.03.90

b) Envelope with 100% of particles

Figure 11:   Beam envelope for a current of 3A (initial emittance 100π mm mrad)

1E-3
50.
40.
30.
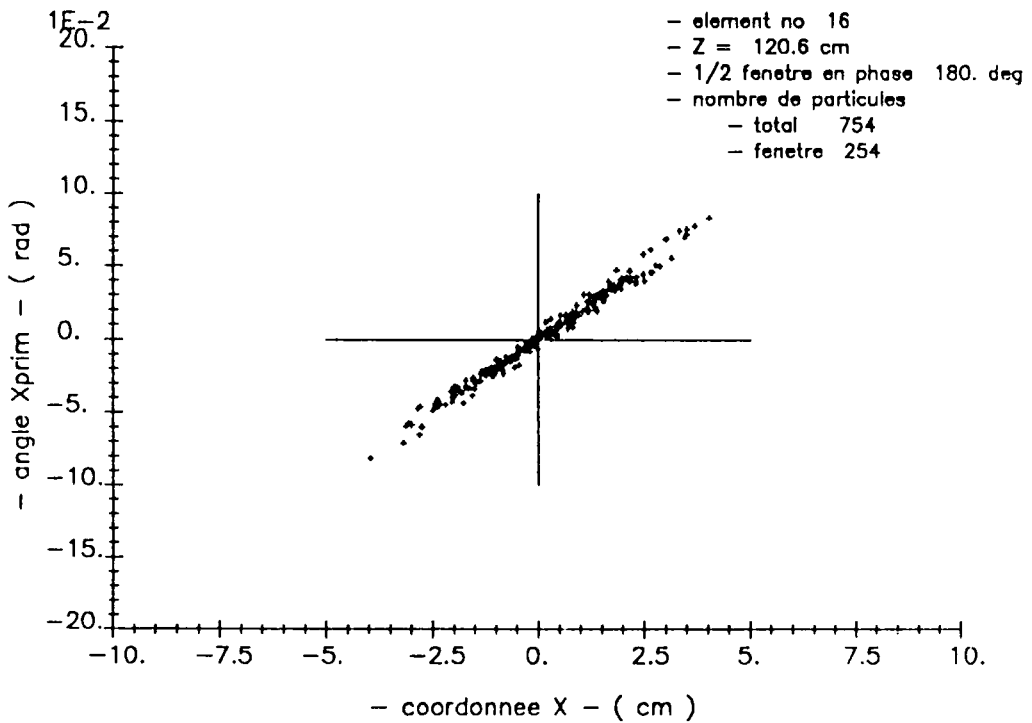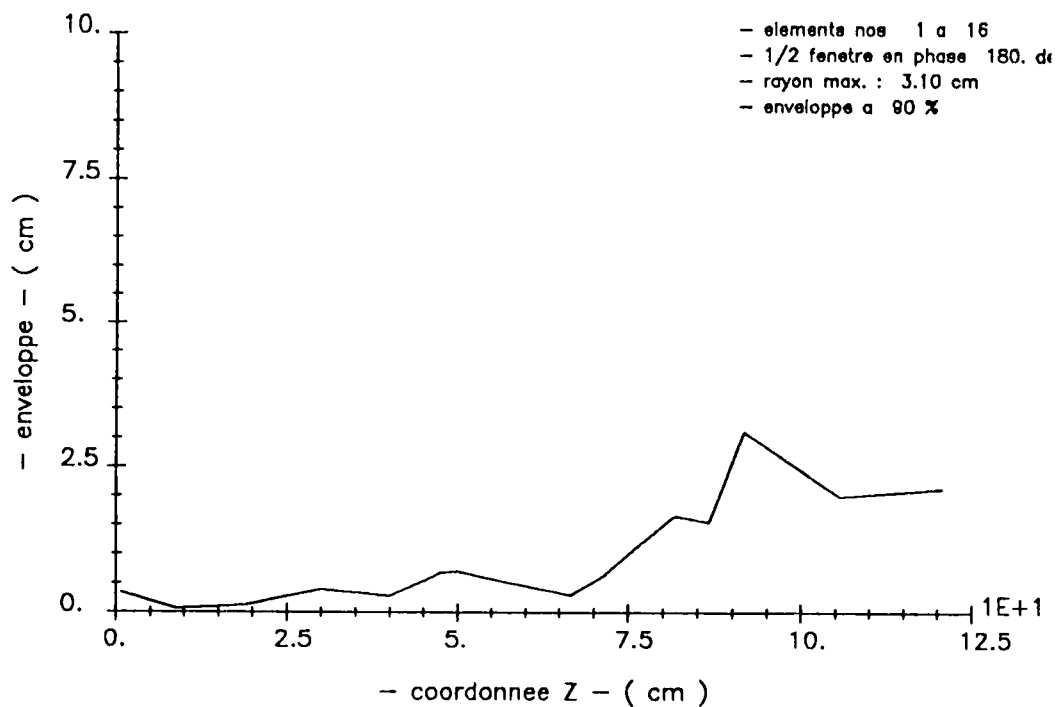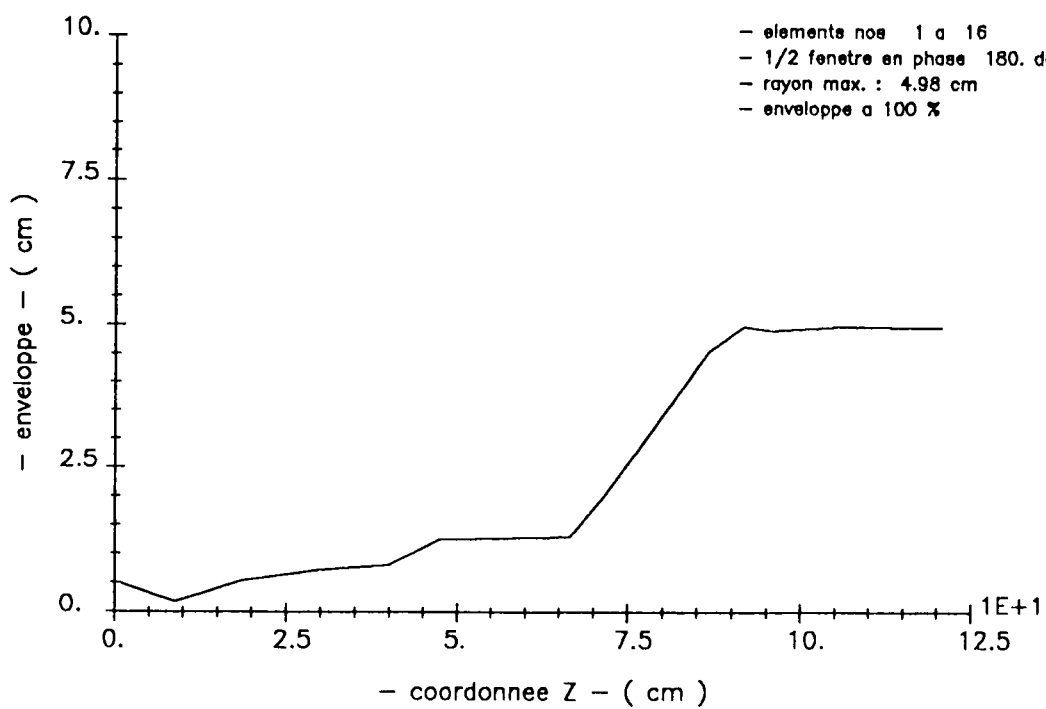20.
10.
0.
-10.
-20.
-30.
-40.
-50.

- angle Xprim - (rad)

- element no   1
- Z =   0.8 cm
- 1/2 fenetre en phase 180. deg
- nombre de particules
      - total   668
      - fenetre 667

-10.   -7.5   -5.   -2.5   0.   2.5   5.   7.5   10.   1E-1

- coordonnee X - (cm)

26.03.90

1E-2
20.
15.
10.
5.
0.
-5.
-10.
-15.
-20.

- angle Xprim - (rad)

- element no   16
- Z =   120.6 cm
- 1/2 fenetre en phase 180. deg
- nombre de particules
      - total   754
      - fenetre 254

-10.   -7.5   -5.   -2.5   0.   2.5   5.   7.5   10.

- coordonnee X - (cm)

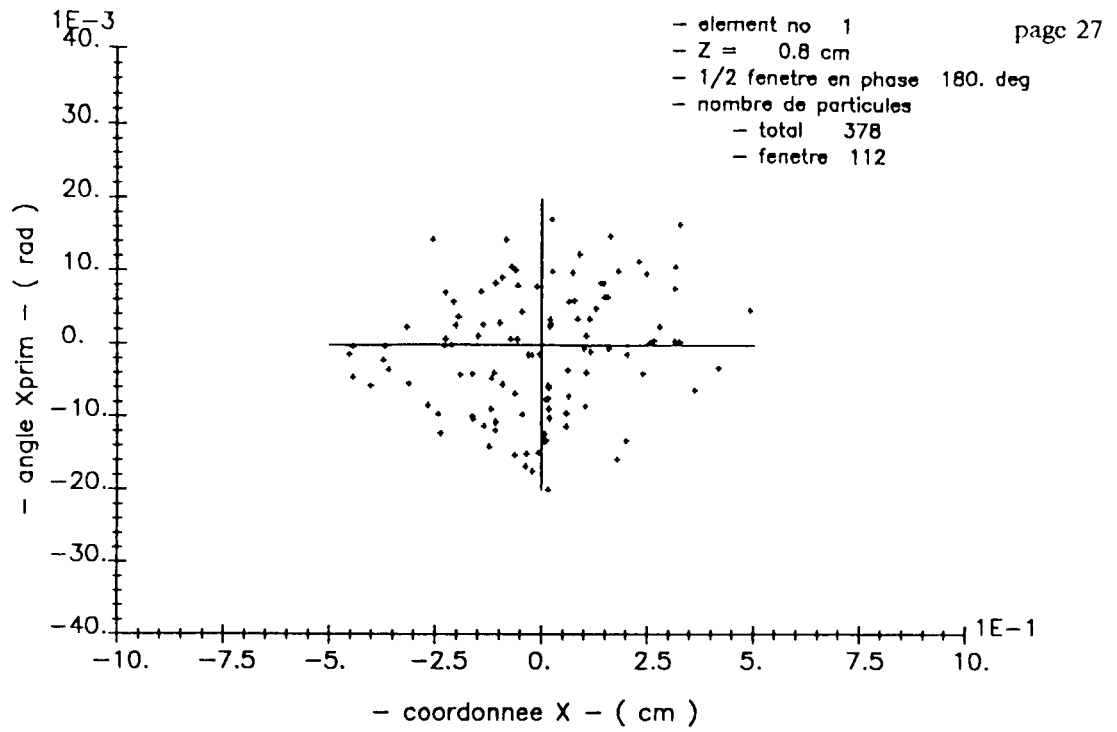*Figure 12*:   Initial and final transverse phase-plane for a current of 3A (initial emittance 100π mm mrad)

a) Envelope with 90% of particles

b) Envelope with 100% of particles

Figure 13: Beam envelope for a current of 10A (initial emittance 100π mm mrad)
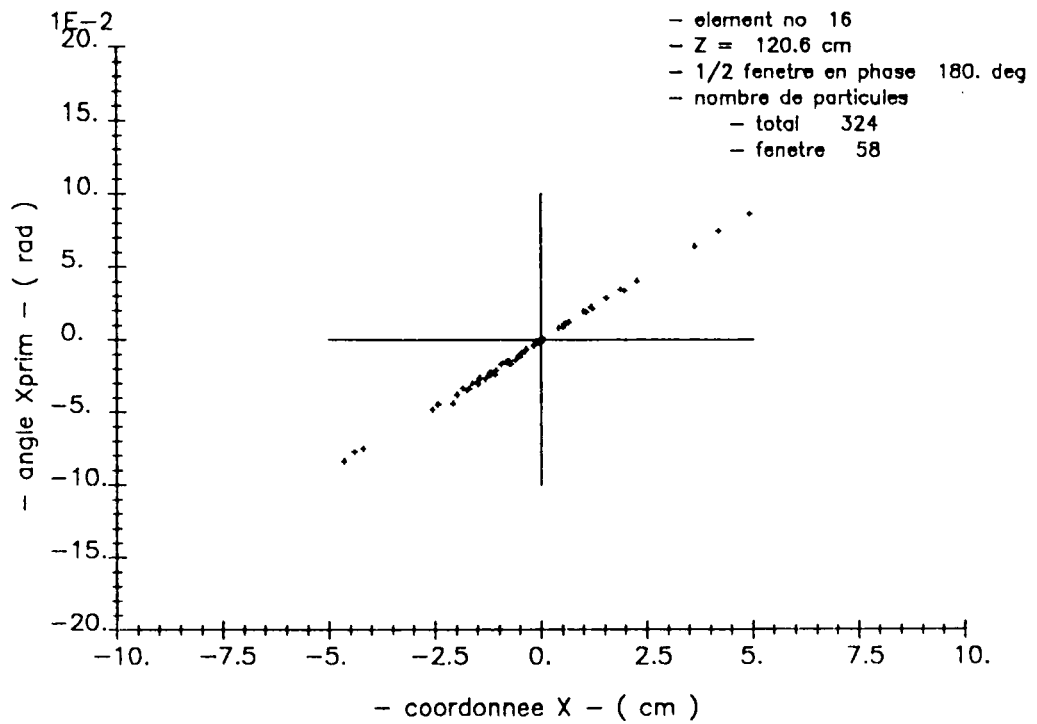
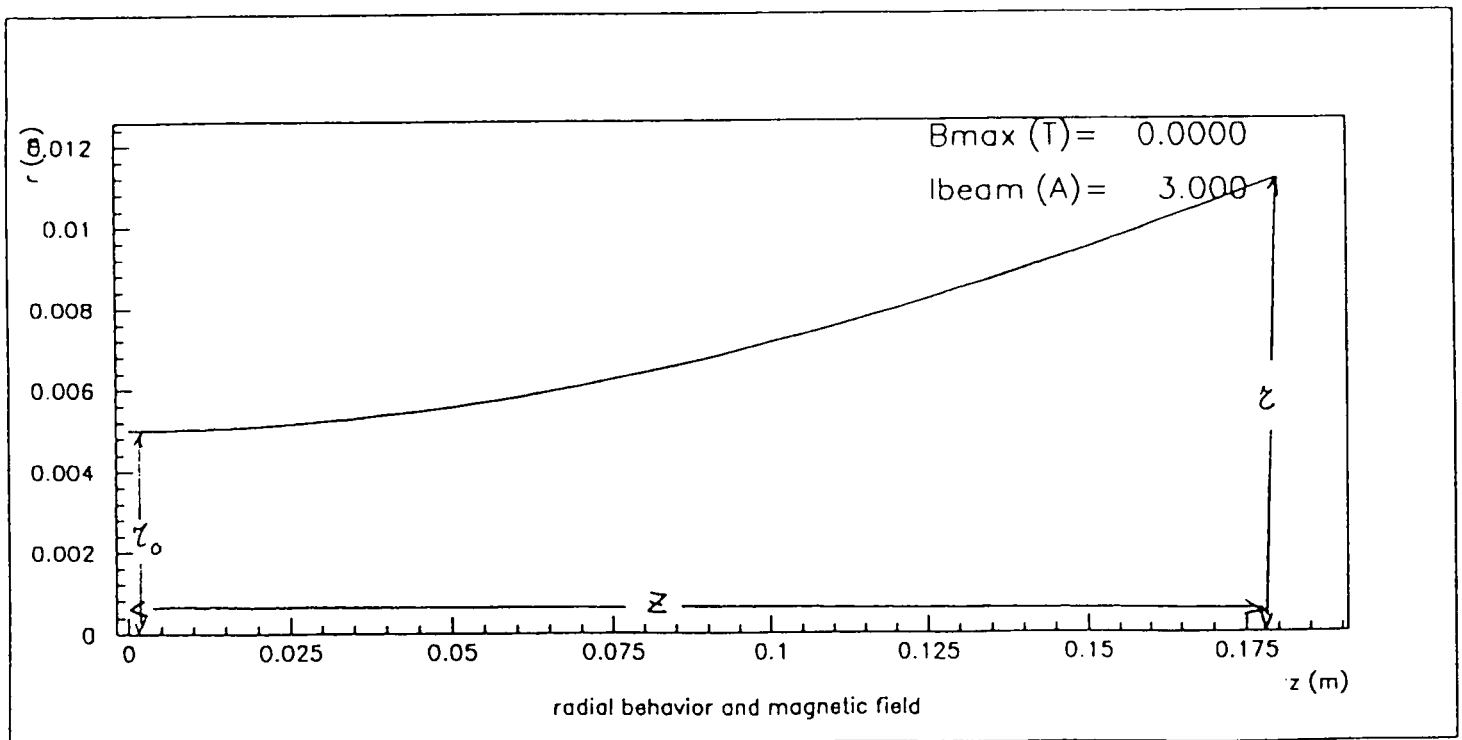*Figure 14:* Initial and final transverse phase-plane for a current of 10A (initial emittance 100π mm mrad).

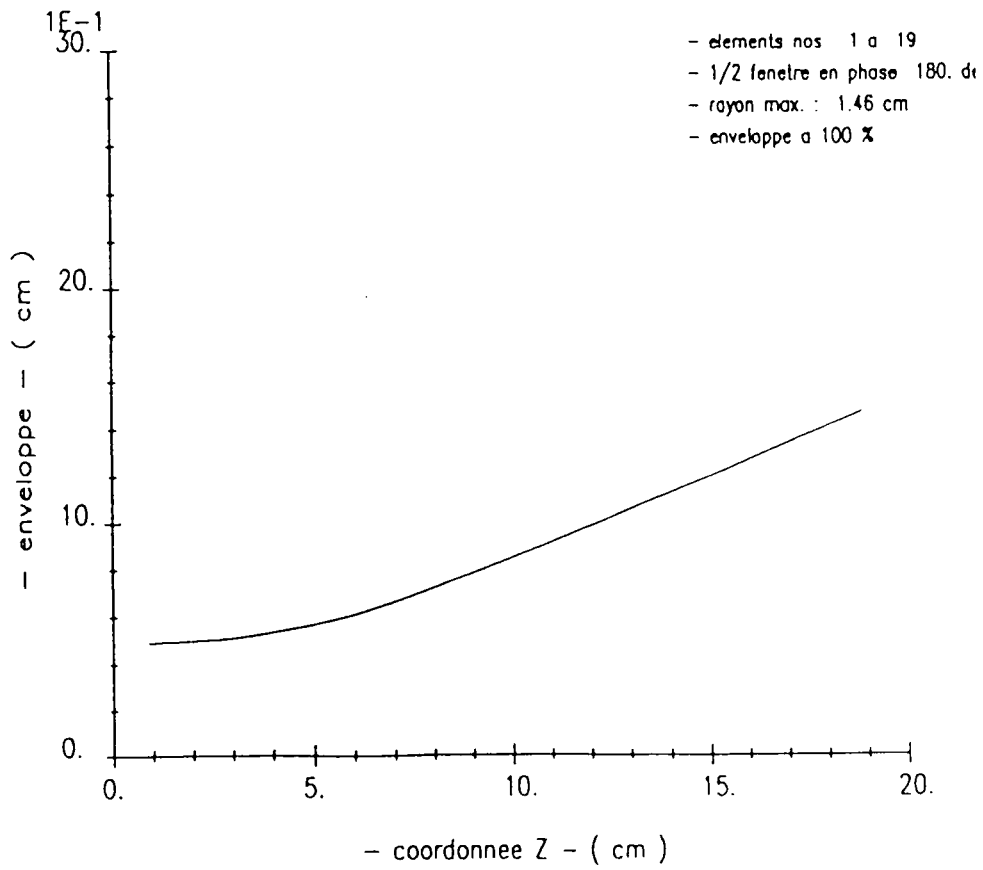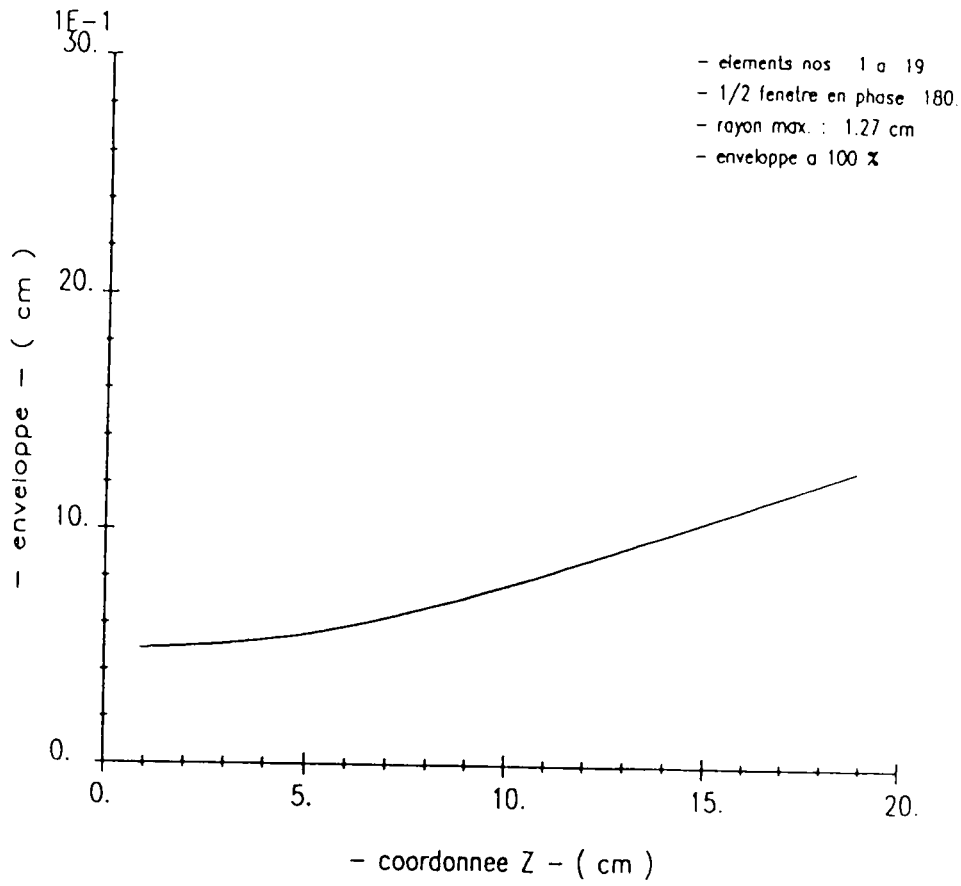*Figure 15:*   Envelope in a drift space in laminar hypothesis (SOLOPT).

- coordonnee Z - (cm)

- elements nos   1 a 19
- 1/2 fenetre en phase 180. d(
- rayon max. : 1.46 cm
- enveloppe a 100 %

- coordonnee Z - (cm)

Figure 16: Envelopes in a drift space calculated with PARMELA for 20π and 200π mm mrad initial emittances.
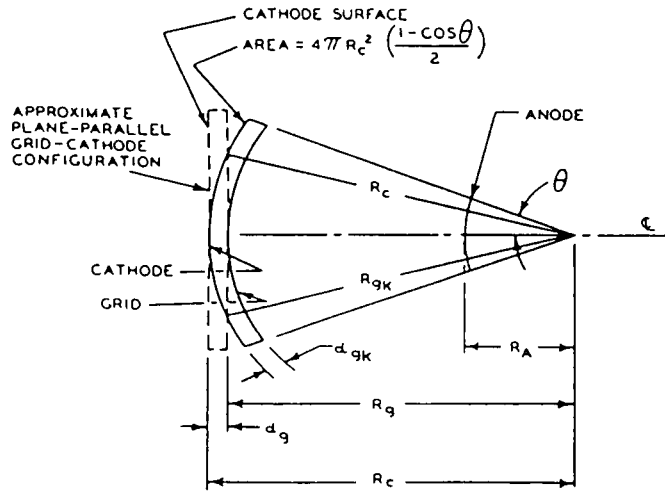
Figure 17: Lay-out of a spherical cathode and planar plate approximation.
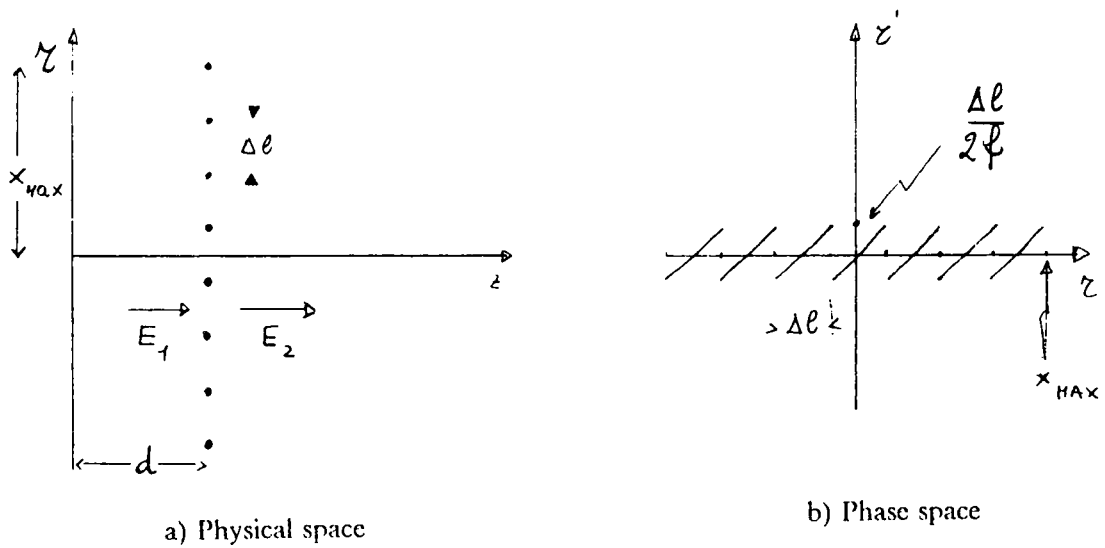

a) Physical space

b) Phase space

Figure 18: Sketch of the emittance generation at the grid.